ITERATIVE BUILDING RECONSTRUCTION FROM MULTI-ASPECT INSAR DATA

U. Soergel, U. Thoennessen, U. Stilla

FGAN-FOM Research Institute for Optronics and Pattern Recognition
76275 Ettlingen, Germany
soe@fom.fgan.de

Commission III, WG III

KEY WORDS: SAR, Building, Detection, Reconstruction, Urban, Simulation, Fusion

ABSTRACT:

The improved ground resolution of state of the art synthetic aperture radar (SAR) sensors suggests using this technique for the analysis of urban areas. The quality of building reconstruction results from SAR or InSAR data is limited by phenomena caused form the inherent oblique scene illumination of SAR sensors. Geometric constraints of the impact of the mentioned SAR phenomena on the visibility of buildings are derived. Especially in dense inner city areas with tall buildings the building reconstruction is often impossible if only a single measurement is available. For rural scenes, suburban areas or industrial plants with large and detached buildings better results can be achieved. The reconstruction quality can be improved in any case by a combined analysis of multi-aspect data. In this paper an approach for the detection and reconstruction of buildings from several InSAR data sets is proposed. The analysis is carried out in an iterative manner. Intermediate results are used as basis for simulations of InSAR data. The simulation results are compared with real imagery. Deviations between the simulations and the real data are eliminated step-by-step. The approach is demonstrated for a multi-aspect InSAR data set of a building group in a rural environment.

1. INTRODUCTION

Three-dimensional city models are of great interest for visualisation, simulation and monitoring purposes in different fields. Such 3D city models are usually derived from aerial imagery (Henricsson, 1996) or LIDAR data (Stilla and Jurkiewicz, 1999; Weidner and Foerstner, 1995). The increasing resolution of SAR sensors opens the possibility to utilize such data for scene interpretation in urban areas as well. Approaches for a 3D building recognition from SAR and InSAR data have been proposed (Bolter, 2001; Gamba et al., 2000; Soergel et al., 2001). Different SAR specific phenomena (Schreier, 1993) like foreshortening, layover, shadow, and multipath-propagation burden the scene interpretation or make it even impossible. These phenomena arise from the side-looking scene illumination of SAR sensors. Especially in dense built-up areas with high buildings, large portions of the data can be interfered by these illumination effects. The analysis of multi-aspect data offers the opportunity to alleviate these drawbacks, e.g. by filling occluded areas with data from other aspect directions.

For the building recognition task the typical appearance of buildings in the InSAR data is modelled. Their height and roof structure can be derived from the InSAR DEM or from the length and the size of the occluded shadow area cast from the building on the ground behind in the intensity image. Other hints to buildings are layover areas and bright double-bounce scatterers at the building footprint. Such context knowledge is exploited by a novel model-based iterative approach to detect and reconstruct buildings presented in this paper. Additionally, a geometric and topologic building model is required for the analysis, e.g. the preferred right-angled geometry of building structures. Besides simple buildings with rectangular footprint more complex footprint structures are considered as well.

In order to consider neighbourhood relations an iterative approach is advantageous. Intermediate reconstruction results are used as reference for a simulation of InSAR data with respect to the parameters of the given real data. Differences between the simulated and the real data control the iterative improvement of the reconstruction.
In Chapter 2 the SAR and InSAR techniques are introduced briefly. The appearance of buildings in the radar imagery is discussed in Chapter 3. Phenomena caused by side-looking illumination are explained and geometric relations for the determination of disturbed data are derived. The model-based approach for the detection and reconstruction of buildings is proposed and demonstrated in Chapter 4.

2. INSAR DATA

Side-looking SAR sensors are mounted on satellites or airplanes. The basic sensor principle is to illuminate large areas on the ground with the radar signal and to sample the backscatter. From the different time-of-flight of the incoming signal the range between the sensor and the scene objects is obtained. The analysis of single SAR images is usually restricted to the signal amplitude.

For interferometric SAR processing (InSAR) two SAR images are required, which were taken from different positions (Bamler and Hartl, 1998). Due to the geometric displacement, the distances from the sensors to the scene differ, which results in a phase difference in the interferogram. Elevation differences in the scene are approximated by a linear function with these phase differences.

The accuracy of an InSAR DEM varies locally depending on the signal to noise ratio (SNR). The so-called coherence is a measure of the local SNR. Coherence is usually estimated from the data by a window-based computation of the magnitude of the complex cross-correlation coefficient of the SAR images. The noise sensitivity results often in `data holes´ or competing elevation values after the geocoding step with a forward transformation. Hence, the InSAR DEM data has to be further processed before the geocoding step is carried out.

In Figure 1 a small part of an InSAR data set of the test site measured from north is illustrated in the original slant range projection. The scene contains several buildings of different types in a rural area close to Solothurn, Switzerland. The ground truth data consisting of a LIDAR DEM and building footprints are shown in Figure 1d. The InSAR data were recorded by the airborne DO-SAR system (Faller and Meier, 1993). The center frequency of this X-band system is 9.5 GHz ($\lambda \approx 3$cm). The slant range data have a resolution of about 1.2m x 1.2m. Range direction is from top to down. Assuming a constant noise power, it is evident that in areas of the intensity image with low backscatter power (dark regions in Figure 1a) the SNR is poor. This results in low coherence (dark regions in Figure 1c) and distorted height data (Figure 1b). A standard deviation of the height data of about 1 m was estimated from a large flat grass area outside the presented area of the scene. Two additional InSAR data sets of the same scene were available, which have been acquired from south with two different off-nadir angles (Figure 1e,f).

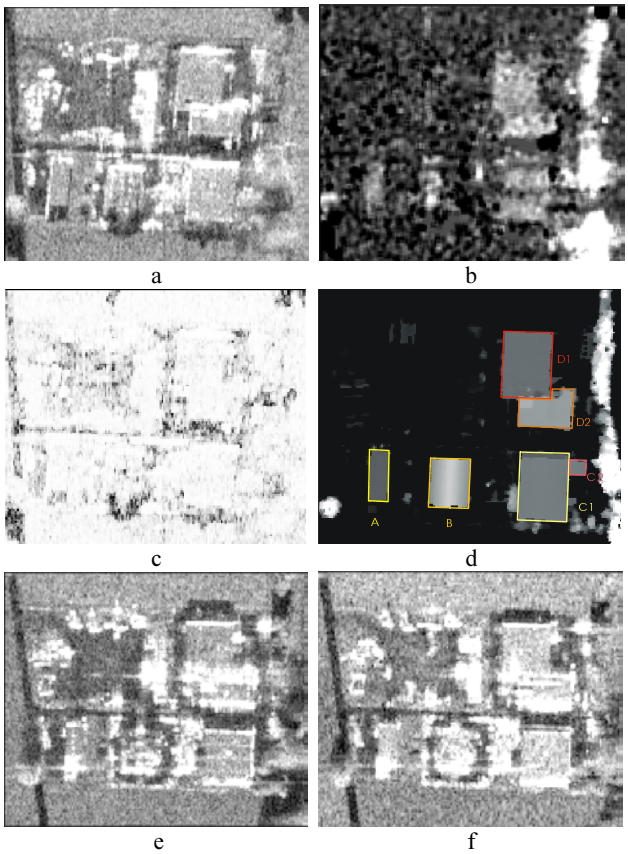

Figure 1. Test data set Solothurn. a-c) InSAR illumination from north (a) intensity, b) DEM, c) coherence); d) ground truth: LIDAR data and building footprints; e,f) intensity of InSAR measurements from south with large (e) and small (f) off-nadir angle.

3. APPEARANCE OF BUILDINGS IN SAR IMAGES

3.1 Phenomena caused by side-looking illumination

Figure 2 illustrates typical effects in SAR images in the vicinity of buildings. The so-called layover phenomenon occurs at locations with steep elevation gradient facing towards the sensor, like vertical building walls (Figure 2a). If object areas located at different positions have the same distance to the sensor, like roofs (I), walls (II), and the ground in front of buildings (III), the backscatter is integrated to the same range cell. Layover areas appear bright in the SAR image (Figure 2 c).

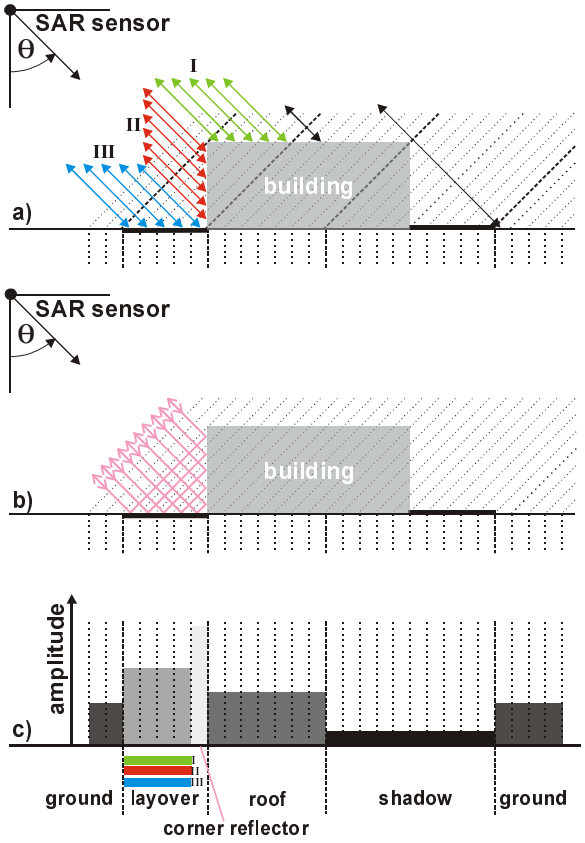

Figure 2. SAR Phenomena at a flat roofed building. a) layover, b) corner reflector, c) range line of SAR image.

Perpendicular alignment of building faces towards the sensor leads to strong signal responses by double-bounce scattering at the dihedral corner reflector between the ground and the building wall (Figure 2b). This results in a line of bright scattering in azimuth direction at the building footprint (Figure 2c). At the opposite building side the ground is partly occluded from the building shadow. This region appears dark in the SAR image, because no signal returns into the related range bins.

Some of the mentioned effects can be studied in Figure 1 comparing the intensity images taken from different directions. The locations of shadow areas on the one hand and layover areas together with bright lines of scattering on the other hand are exchanged comparing the acquisition from north (Figure 1a) with the two acquisitions from south (Figure 1e,f). In case of the latter ones the length of the shadow areas differ due to the variation of the viewing angle θ (off-nadir angle).

3.2 Geometric Constraints

In this section the phenomena of layover and shadow are discussed in more detail. The sizes of the layover areas l_g and shadow areas s_g on the ground in range direction depend on the viewing angle θ and the building height h. The layover area (see Figure 3a) is given by:

$$l_g = h \cdot \cot(\theta). \quad (1)$$

For the building analysis the roof area l_{rf} is of interest, which is influenced by layover. At the far side of a building with width w a part of the roof is not interfered with layover (shown in green in Figure 3a), if the inequation is fulfilled:

$$h < w \cdot \tan(\theta). \quad (2)$$

In case of shadow geometric relations can be obtained, too (Figure 3b). The slant range shadow length Δr is the hypotenuse of the right-angled triangle with the two sides h and s_g. Hence, the building elevation h is given by:

$$h = \Delta r \cdot \cos(\theta). \quad (3)$$

A simple projection of the slant range SAR data on a flat ground plane (ground range), ignoring the building elevation, leads to a wrong mapping of the roofs edge r_1 to point r_1'. Starting from point r_2 the true position x_1 of the building wall can be determined (Bolter, 2001):

$$x_2 = r_2 \cdot \sin(\theta) \quad (4)$$

$$x_1 = x_2 - \Delta r \cdot \sin(\theta) \quad (5)$$

$$s_g = x_2 - x_1 = h \cdot \tan(\theta). \quad (6)$$

However, the shadow analysis can be reliable only, if the ground behind the building is flat and if no signal from other elevated objects interferes the shadow area (e.g. a neighboured building).

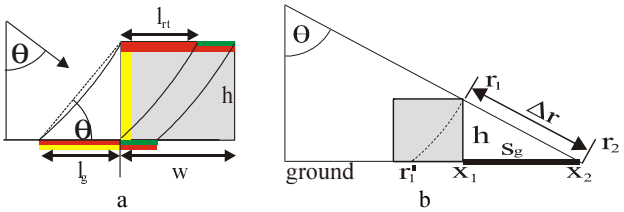

Figure 3. a) Layover in front and on a flat roofed building, b) Shadow behind a building.

Different building roof structures lead to special shapes of the shadow cast on the ground. The sketch in Fig. 7 illustrates the appearances of common building roof types in SAR amplitude or intensity images. The assumed illumination direction is from right to left. The shadow shape depends on the aspect. Flat roofed buildings cast usually a stripe-like or L-shaped shadow. A building with pent roof structure (sloped roof) may cause a trapezoidal shadow. A gabled roof building may cast sexangle shaped shadow. But, both of the latter building types may cast a stripe-like or L-shaped shadow as well (e.g. if the range direction is top-down or bottom-up in Figure 4).

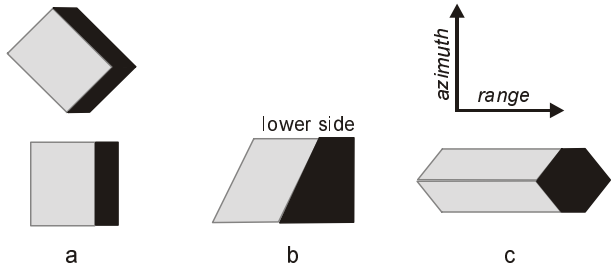

Figure 4. Appearance of different buildings types in SAR amplitude or intensity images: a) flat roof, b) pent roof, c) gable roof.

3.3 Simulation of layover, shadow and dominant scattering

Based on a ground truth DEM layover and shadow areas can be simulated (Meier et al., 1993) as well as dominant scattering (Soergel et al., 2002). SAR simulation techniques are incorporated in the iterative building detection and reconstruction approach presented in the next chapter.

4. APPROACH FOR BUILDING DETECTION AND RECONSTRUCTION FROM INSAR DATA

4.1 Algorithm overview

The building recognition is performed in an iterative manner. At least one InSAR data set is required. Detection and reconstruction of buildings are carried out in separated modules. The first step is the pre-processing of the InSAR data, e.g. smoothing and speckle reduction (Desnos and Matteini, 1993). In the subsequent segmentation step primitive objects are extracted from the original slant range InSAR data. This is advantageous in order to avoid artefacts due to the geocoding, e.g. the distorted appearance of building edges in the ground range projection. From primitive objects more complex objects (building hypotheses) are assembled in the detection module.

After projection of coordinates of these building candidates from slant range into the world coordinate system, a building recognition step follows. In this module model knowledge is exploited, e.g. the rectangular shape of buildings or their preferred parallel alignment along roads. If multi-aspect data are available, the sets of building candidates derived from the different data sets are fused.

Intermediate results are used for a simulation of the InSAR DEM, layover, shadow, and dihedral corner reflectors. The simulation results are re-projected to the SAR geometry and compared with the real data. Differences between the simulation and the real data control the update of the process: new building hypotheses are generated and false ones eliminated. Hence, the resulting scene description is expected to converge to the real 3D objects in the scene with increasing number of cycles. The processing stops either after a given maximum number of iterations or if the RMS of the difference between the simulated and the real InSAR DEM is smaller than a given threshold.

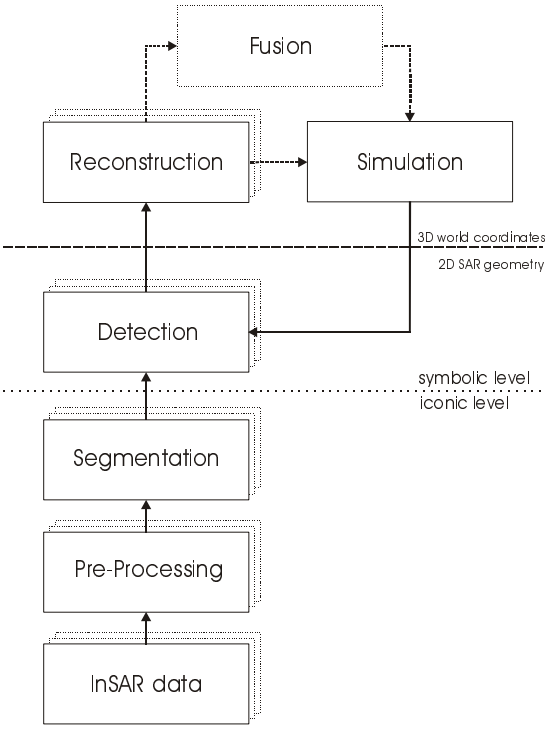

Figure 5. Workflow of building reconstruction.

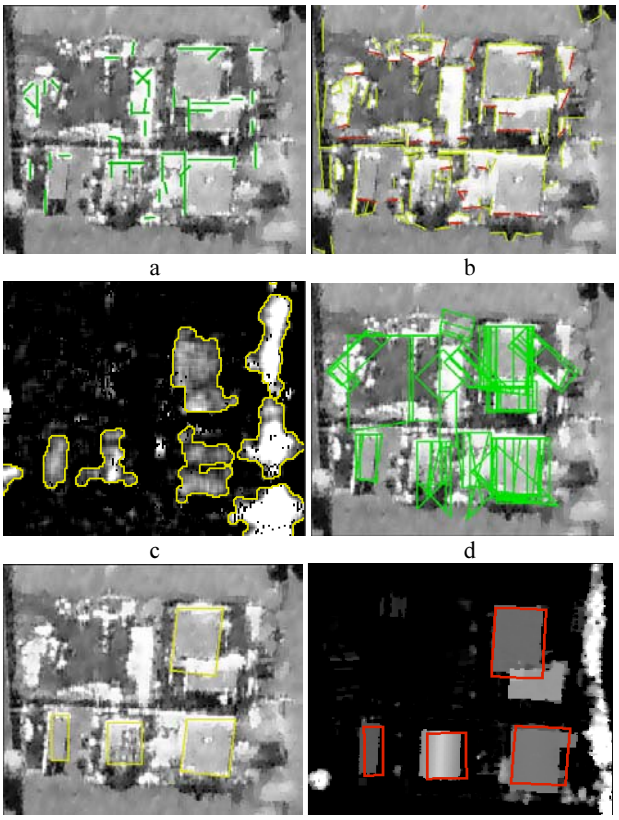

Figure 6. Generated Objects: a) STRONG_SCATTER_LINE; b) NEAR_SHADOW_EDGE (red), FAR_SHADOW_EDGE (yellow); c) ELEVATED_REGION; d) QUADRANGLE; e) BUILDING_CANDIDATE; f) reconstructed footprints overlaid on LIDAR reference DEM.

4.2 Segmentation of primitive objects

Primitive objects are segmented independently in the intensity and the height data. In the first case edges are detected, which may coincide with the building boundaries and the shadow cast from the building. In the latter case connected elevated structures are segmented.

4.2.1 Intensity Data: In the intensity data three types of edge and line structures are detected:

- Salient bright lines caused from layover or double-bounce reflection. These objects will be referred as objects STRONG_SCATTER_LINE. The segmentation is carried out by a morphologic thinning of connected, elongated, and bright segments, which were derived by thresholding the intensity image. The generated objects are shown in Figure 6a superimposed on the speckle filtered intensity image.
- Edge structures at the border of a dark region, which are potentially caused from building shadow. The edges are segmented in two different manners. The first way is applying an edge detector (Canny, 1986). However, despite a preceding speckle filtering step object edges appear often disturbed in SAR images. Hence, a second set of edges is segmented by approximating the borders of dark regions with lines. These two sets of edges are merged. Two different kinds of primitive objects are distinguished. The first set build those border edges of the dark region, which face the sensor (object NEAR_SHADOW_EDGE, red in Figure 6b). The other set consists of the edges at the far side of the dark region (object FAR_SHADOW_EDGE, yellow in Figure 6b).
- The remaining edges (not shown here) build the set of other objects BUILDING_EDGE. Those may coincide with building edges orientated in range direction.

4.2.2 Height Data: In the height data a segmentation of objects with significant elevation above ground is carried out. For this purpose a normalized DEM (NDEM) is derived from the InSAR height data, which represents the elevation of objects over ground. First a rank filtering of the height data is performed (Eckstein and Munkelt, 1995). Such filtering is especially feasible in case of a rather flat terrain like in the test area. The filter window size is chosen larger than the expected maximum building area. Height values coinciding with poor coherence or low intensity are not considered in this step in order to exclude blunders. One parameter of the rank filter is the position of the returned element from the bottom-up ordered elevation values. This parameter is adjusted according to the mean coherence of the scene. The filtering results in a digital terrain model (DTM) representing the topography without elevated objects like trees or buildings. The NDEM is derived from the difference of the original InSAR DEM to the DTM. Using an elevation threshold elevated objects are separated from the ground in the NDEM. Connected regions of elevated pixels build the set of objects ELEVATED_REGION. The regions segmented in the test data are drawn in Figure 6c in yellow. The segments coincide with the building locations and groups of trees (on the right).

4.3 Detection of Building Candidates in the Slant Range

From the line and edge structured primitive objects more complex objects QUADRANGLE are assembled by a production system (Niemann, 1990):

- At least one edge of the object QUADRANGLE facing the sensor must be derived from an object STRONG-SCATTER_LINE.
- Analogous, an object NEAR_SHADOW_EDGE is required at the far edges of the object QUADRANGLE.

The objects QUADRANGLE from the test data are shown in Figure 6d. Only a subset of those coincides actually with buildings. A variety of different object configurations are source of false hints, e.g. fences or car rows etc. For the discrimination of buildings from the rest the objects ELEVATED_REGION are used. The intersection area of each object QUADRANGLE with all objects ELEVATED_REGION is determined. The ratio of the intersection area to the quadrangle area is used as object feature "elevated area ratio". Only objects QUADRANGLE with a high-elevated area ratio are considered as objects BUILDING-CANDIDATE. The number of objects BUILDING_CANDIDATE is further reduced: from mutual intersecting candidates only the best assessed one is considered for the reconstruction step in this iteration. The assessment value depends on:

- the overlap and the parallelism of the primitive objects.
- the feature "elevated area ratio".

In Figure 6e the remaining objects BUILDING_CANDIDATE of the first iteration are drawn in yellow.

4.4 Building Reconstruction

The building reconstruction is based on the following assumptions:

- Footprints of buildings have rectangular or right-angled shape.
- Buildings are elevated objects with different roof structures. Three types of parametric roof models are considered: flat roof, gabled roof and pent roof. A common feature of the parametric building models is the rectangular footprint.
- A generic building model addresses complex buildings structures, which consist of several parts like wings. These parts may have different height for each part. The footprint of a generic building is modelled as a right-angled polygon. The number of parts of a generic object is not a-priori determined.
- Neighboured buildings and the parts of complex buildings have often the same orientation, because they are aligned parallel to roads.

For the reconstruction step the coordinates of the objects BUILDING_CANDIDATE are transformed from the SAR geometry into the world coordinate system. This step requires knowledge of the object height. A pixel-by-pixel transformation leads to distorted object edges due to the noise sensitivity of the interferometric measurement. Averaging the height values inside the borders of each object BUILDING_CANDIDATE reduces the noise impact. In case of a flat roofed building, the average value is the optimal estimate of the building height. In order to consider the different reliability of the height pixel values, the related coherence value is used as weight in the averaging procedure.
Because of tolerances in the building candidates assembly, the building footprint is usually not right-angled after geocoding. Therefore, the footprint is approximated by a rectangular or right-angled polygon. The roof structure is analysed with two different methods. The first method is restricted to the height data. After the re-projection of the right-angled building into the slant range, planes are fitted to the data. A figure of merit (FoM) is calculated from the RMS of the fitted planes with the data. The second method analyses size and shape of the shadow areas (objects NEAR_SHADOW_EDGE and FAR_SHADOW-EDGE). In this case a figure of merit is derived from the overlap of the detected objects FAR_SHADOW_EDGE with the shadow area. If one of the two FoMs is significantly better, the related reconstruction is chosen. In case of comparable FoM, an adjustment step is carried out to determine the roof shape and to improve the footprint location. The corrected footprint and roof structure are features of new produced objects BUILDING.

4.5 Iterative improvement of the results

The first iteration is restricted to the reconstruction of objects BUILDING with rectangular footprints (Figure 6f). In the following iterations the generic building model is considered as well. Due to parameter tolerances, the reconstructed orientations of neighboured objects BUILDING might differ slightly. Hence, the orientations are corrected. The assessment of the objects buildings is used as weight for this adjustment step. Based on the intermediate results simulations of InSAR NDEM data, layover, shadow, and dihedral corner reflectors are carried out with respect of the parameters of the real data. Figure 7a shows the result of the simulation after the first iteration. Differences between the simulated and the real slant range NDEM data are hints to inconsistencies. These govern the update of the process: new building hypotheses are generated and false ones eliminated. Then the reconstruction step is repeated. The iteration stops if the overall RMS between the simulated and the real height data falls below a threshold or if a given number of cycles have been carried out. The final result will be the reconstruction, which minimized the mentioned overall RMS. The difference image of simulated and real NDEM for the test data is depicted in Figure 7b. If the reconstructed elevation is higher than the real data, bright areas are the consequence. If the real NDEM is higher, dark regions appear (e.g. at the trees on the right).

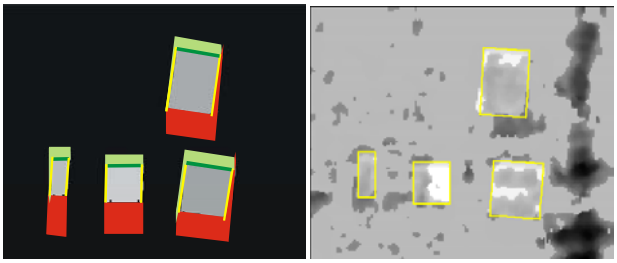

a b

Figure 7. a) Simulation result (slant range): Elevation (grey), layover (pale green), corner reflector (dark green), shadow (red), and other building edges (yellow); b) difference image of simulated and real NDEM

4.6 Analysis of multi-aspect data

If several InSAR data sets are analysed, the results are fused. Occluded areas are filled and layover effects compensated. In case of a multi-aspect analysis an iterative approach is particularly suitable, because hints from the one image may initiate a refined analysis at the related locations in the other images. Figure 8 illustrates this for the test data set. The resulting building footprints after the first process cycle are depicted overlaid on the intensity data in Figures 8a-c in ground

range projection. The fused objects BUILDING-CANDIDATE are shown in Figure 8d. Building *B* was not detected in case of the data set measured from south with small viewing angle (Figure 8c). The fusion offers the opportunity to refine the analysis at this location in this data set, too. If competing building candidates were generated in the different data sets a choice has to be made. This choice is driven by the assessment of the candidates. If one candidate shows a significant better assessment than the others it is chosen for the fused result. In case of candidates with comparable assessment a new candidate is calculated from the given ones by an adjustment procedure. The assessment of the original candidates serves as weights for this adjustment.

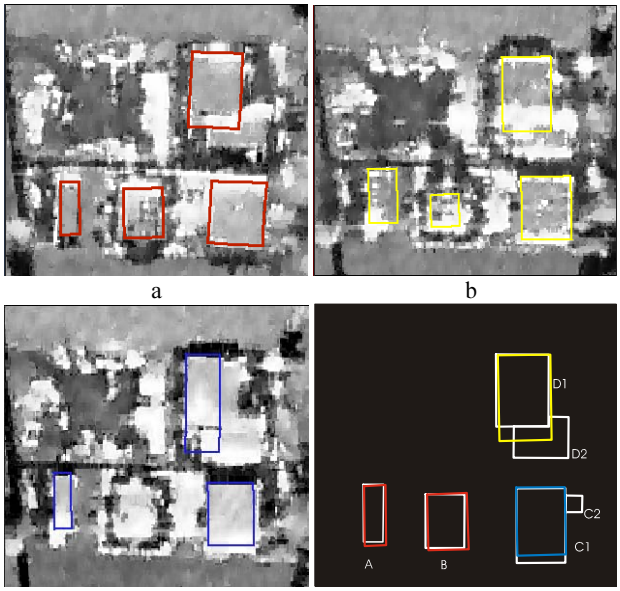

Figure 8. Multi-aspect analysis after the first iteration: a), objects BUILDING_CANDIDATE for the data set acquired from north overlaid on intensity in ground range; b,c) like a) for illumination from south with large (b) and small (c) viewing angle; d) fused set of objects BUILDING_CANDIDATE.

5. RESULTS

In Figure 9a the result of an analysis based alone on the data set acquired from the north direction after three iterations is shown in red. The ground truth building footprints are depicted in white. No false positives have been detected. All the detected buildings were reconstructed as flat roof buildings. Due to disturbed height data (see Figure 1b) – probably caused by dominant scattering – the building *B* was not reconstructed correctly. The small building part *C2* of the building group *C* was not detected. But, this building part is not detectable in the data even for a human observer. Both elements of the building group *D* were detected. However, the reconstruction of the footprints was topologically incorrect (rectangular building *D1* was reconstructed with a small annex and the annex of building *D2* is missing). But the affected building area is small in both cases.

The result of the multi-aspect analysis is illustrated in Figure 9b. The main improvement is that building B was now detected properly and reconstructed correctly as gabled roof building. The roof structure was derived mainly from the shadow analysis in this case. A 3D visualisation of this result is shown in Figure 9c together with surrounding trees from the InSAR NDEM. The RMS of the corners of the building footprints is smaller than 3 m in x and y direction. The RMS of the mean elevation is about 1.5 m. Figure 9d depicts the reconstructed buildings (grey) superimposed with the LIDAR data (green).

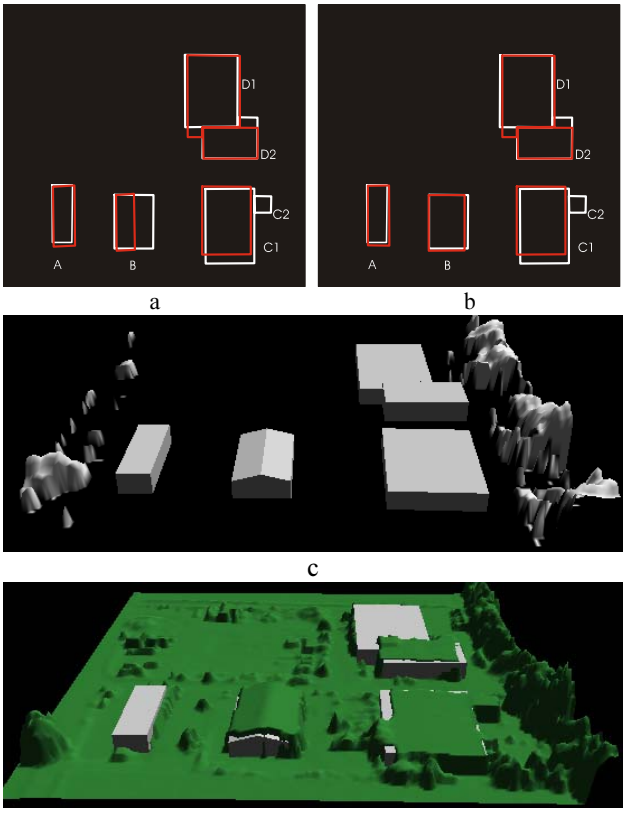

Figure 9. Final results: a) analysis of data set measured from north alone; b) result for multi-aspect data; 3D visualisation of b) with surrounding trees; reconstructed buildings (grey) superimposed with the LIDAR data in green.

6. CONCLUSION

The side-looking sensor principle of SAR is disadvantageous for the building reconstruction task. Especially in dense urban environments with tall buildings this task is often unfeasible. But, in case of suburban or rural scenes acceptable building reconstruction results can be achieved. Building features are detectable in the InSAR DEM and in the InSAR intensity. The coherence should be considered in order to avoid blunders. Occlusion and layover effects can be compensated by a multi-aspect analysis. This leads to a further improvement of the reconstruction quality. An iterative approach offers the opportunity of a stepwise consideration of the mutual interdependencies of the man-made objects. Furthermore, the evidence of building candidates is enhanced by a confirmation from analysis results of several data sets.

ACKNOWLEDGEMENT

We want to thank Dr. Schmid (Swiss Defence Procurement Agency) for providing the InSAR and LIDAR data.

REFERENCES

Bamler R, Hartl P (1998) Synthetic Aperture Radar Interferometry, Inverse problems, Vol. 14, No. 4, pp. 1-54.

Bolter R, Buildings from SAR (2001) Detection and Reconstruction of Buildings from Multiple View High Resolution Interferometric SAR Data. PhD. thesis, University Graz, Austria.

Canny J (1986) A Computational Approach to Edge Detection, IEEE Transactions of Pattern Analysis and Machine Intelligence, Vol. 8, No. 6, pp. 679-698.

Desnos Y L, Matteini. V (1993) Review on structure detection and speckle filtering on ERS-1 images. EARSeL Advances in Remote Sensing, 2(2), pp. 52-65.

Eckstein W and Munkelt O (1995) Extracting Objects from Digital Terrain Models. In: Schenk T (ed.) Remote Sensing and Reconstruction for Three-Dimensional Objects and Scenes, Proc of SPIE 2572, pp. 222-231.

Faller N P, Meier E H (1995) First results with the airborne single-pass DO-SAR interferometer, IEEE Transactions on Geoscience and Remote Sensing, Vol. 33, No. 5, pp. 1230-1237.

Gamba P, Houshmand B, Saccini M (2000) Detection and Extraction of Buildings from Interferometric SAR Data, IEEE Transactions on Geoscience and Remote Sensing, Vol. 38, No. 1, pp. 611-618.

Henricsson O (1996) Analysis of Image Structures using Color Attributes and Similarity Relations, PhD Thesis, ETH Zuerich.

Meier E, Frei U, and Nuesch D (1993) Precise Terrain Corrected Geocoded Images. In: Schreier G (ed.) SAR Geocoding: Data and Systems, Wichmann, Karlsruhe, pp. 173-185.

Niemann H (1990) Pattern Analysis and Understanding, Springer-Verlag, Berlin.

Schreier G (1993) Geometrical Properties of SAR Images. In: Schreier G (ed.) SAR Geocoding: Data and Systems. Wichmann, Karlsruhe, pp. 103-134.

Soergel U, Schulz K, Thoennessen U (2001) Phenomenology-based segmentation of InSAR data for building detection. In: Radig B, Florczyk S (eds.) Pattern Recognition, 23rd DAGM Symposium, Berlin: Springer, pp. 345-352.

Soergel U, Schulz K, Thoennessen U, Stilla U (2002) Utilization of 2D and 3D information for SAR image analysis in dense urban areas. Proc. 4th European conference on synthetic aperture radar, EUSAR 2002. Berlin: VDE, pp. 429-434.

Stilla, U, Jurkiewicz, K (1999) Reconstruction of building models from maps and laser altimeter data. In: Agouris, P., Stefanidis, A. (eds.), Integrated spatial databases: Digital images and GIS, Berlin, Springer, pp. 34-46.

Weidner U, Foerstner W (1995) Towards Automatic Building Extraction from High Resolution Digital Elevation Models, ISPRS Journal, Vol. 50, No. 4, pp. 38--49.